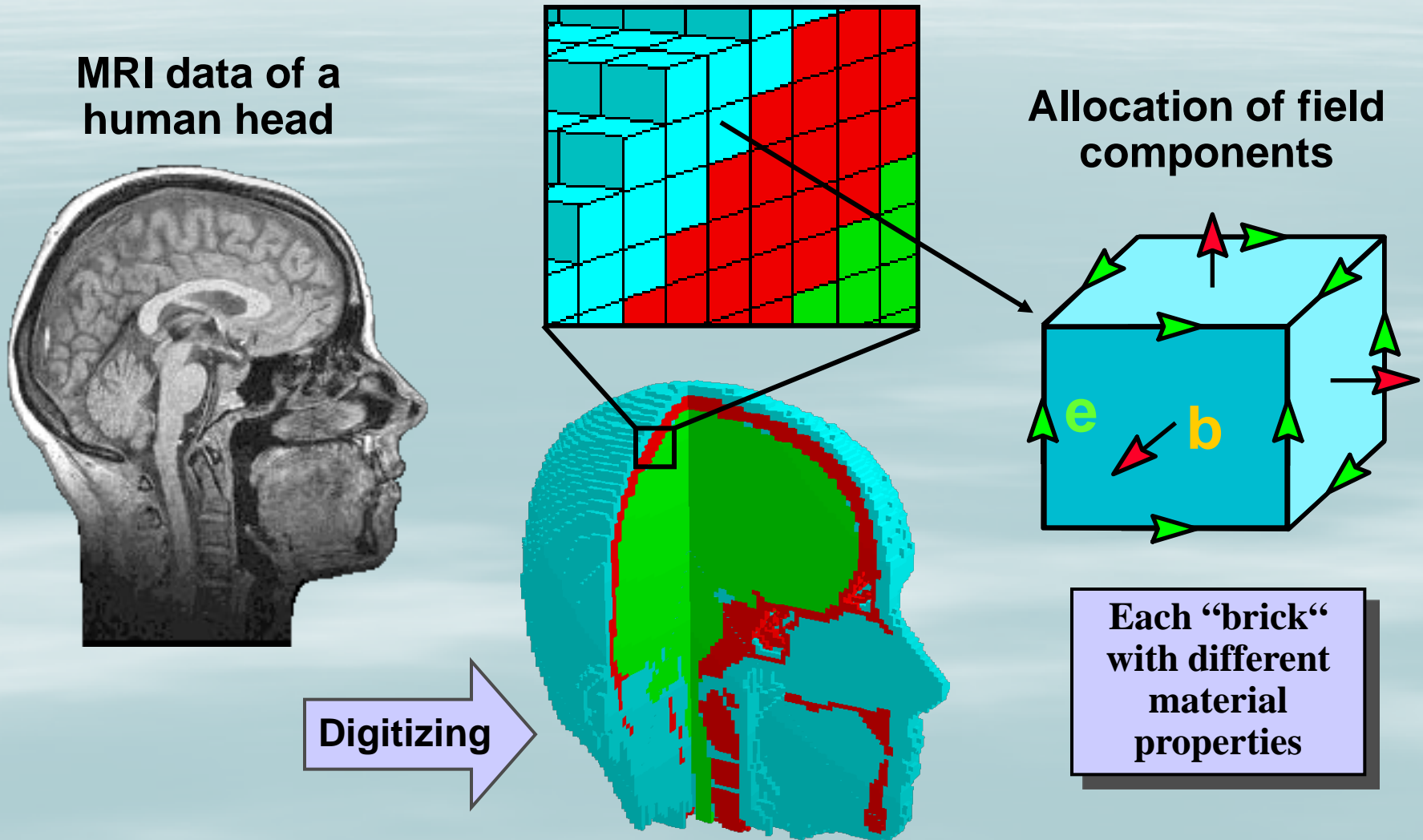


FDTD Basics

USPAS

June, 2010

Finite Difference Gridding



Taylor Expansion

Taylor series
expansions about x_i

$$u(x_i + \Delta x)\Big|_{t_n} = u\Big|_{x_i, t_n} + \Delta x \cdot \frac{\partial u}{\partial x}\Big|_{x_i, t_n} + \frac{(\Delta x)^2}{2} \cdot \frac{\partial^2 u}{\partial x^2}\Big|_{x_i, t_n} \\ + \frac{(\Delta x)^3}{6} \cdot \frac{\partial^3 u}{\partial x^3}\Big|_{x_i, t_n} + \frac{(\Delta x)^4}{24} \cdot \frac{\partial^4 u}{\partial x^4}\Big|_{\xi_1, t_n}$$

$$u(x_i - \Delta x)\Big|_{t_n} = u\Big|_{x_i, t_n} - \Delta x \cdot \frac{\partial u}{\partial x}\Big|_{x_i, t_n} + \frac{(\Delta x)^2}{2} \cdot \frac{\partial^2 u}{\partial x^2}\Big|_{x_i, t_n} \\ - \frac{(\Delta x)^3}{6} \cdot \frac{\partial^3 u}{\partial x^3}\Big|_{x_i, t_n} + \frac{(\Delta x)^4}{24} \cdot \frac{\partial^4 u}{\partial x^4}\Big|_{\xi_2, t_n}$$

Finite Difference: Approximation of Derivatives

Central-difference approximation

$$u(x_i + \Delta x)\Big|_{t_n} + u(x_i - \Delta x)\Big|_{t_n} = 2 \cdot u\Big|_{x_i, t_n} + (\Delta x)^2 \cdot \frac{\partial^2 u}{\partial x^2}\Big|_{x_i, t_n} + \frac{(\Delta x)^4}{12} \cdot \frac{\partial^4 u}{\partial x^4}\Big|_{\xi_3, t_n}$$

2nd derivative of u at spatial location x_i and time t_n

$$\frac{\partial^2 u}{\partial x^2}\Big|_{x_i, t_n} = \left[\frac{u(x_i + \Delta x) - 2 \cdot u(x_i) + u(x_i - \Delta x)}{(\Delta x)^2} \right]_{t_n} + O[(\Delta x)^2]$$

Shorthand notation

$$\frac{\partial^2 u}{\partial x^2}\Big|_{x_i, t_n} = \frac{u_{i+1}^n - 2u_i^n + u_{i-1}^n}{(\Delta x)^2} + O[(\Delta x)^2]$$

Finite Difference: Scalar Wave Equation

$$\frac{\partial^2 u}{\partial t^2} = c^2 \frac{\partial^2 u}{\partial x^2}$$

Scalar wave equation

$$\frac{u_i^{n+1} - 2u_i^n + u_i^{n-1}}{(\Delta t)^2} + O[(\Delta t)^2] = c^2 \left\{ \frac{u_{i+1}^n - 2u_i^n + u_{i-1}^n}{(\Delta x)^2} + O[(\Delta x)^2] \right\}$$

$$u_i^{n+1} \cong (c\Delta t)^2 \left[\frac{u_{i+1}^n - 2u_i^n + u_{i-1}^n}{(\Delta x)^2} \right] + 2u_i^n - u_i^{n-1}$$

FD update
equation for u_i

Maxwell's Equations

- *Faraday's law:*

$$\frac{\partial \mathbf{B}}{\partial t} = -\nabla \times \mathbf{E} - \mathbf{M}$$

$$\frac{\partial}{\partial t} \iint_A \mathbf{B} \cdot d\mathbf{A} = -\oint_L \mathbf{E} \cdot d\mathbf{L} - \iint_A \mathbf{M} \cdot d\mathbf{A}$$

- *Ampere's law:*

$$\frac{\partial \mathbf{D}}{\partial t} = \nabla \times \mathbf{H} - \mathbf{J}$$

$$\frac{\partial}{\partial t} \iint_A \mathbf{D} \cdot d\mathbf{A} = \oint_L \mathbf{H} \cdot d\mathbf{L} - \iint_A \mathbf{J} \cdot d\mathbf{A}$$

- *Gauss' law for electric field:*

$$\nabla \cdot \mathbf{D} = 0$$

$$\oiint_A \mathbf{D} \cdot d\mathbf{A} = 0$$

- *Gauss' law for magnetic field:*

$$\nabla \cdot \mathbf{B} = 0$$

$$\oiint_A \mathbf{B} \cdot d\mathbf{A} = 0$$

Electric and Magnetic fields
coupled in Maxwell's equations

Vector Components of Faraday's and Ampere's Law

Vector components for linear, isotropic, nondispersive, and lossy materials

$$\frac{\partial H_x}{\partial t} = \frac{1}{\mu} \left[\frac{\partial E_y}{\partial z} - \frac{\partial E_z}{\partial y} - (M_{\text{source}_x} + \sigma^* H_x) \right]$$

$$\frac{\partial H_y}{\partial t} = \frac{1}{\mu} \left[\frac{\partial E_z}{\partial x} - \frac{\partial E_x}{\partial z} - (M_{\text{source}_y} + \sigma^* H_y) \right]$$

$$\frac{\partial H_z}{\partial t} = \frac{1}{\mu} \left[\frac{\partial E_x}{\partial y} - \frac{\partial E_y}{\partial x} - (M_{\text{source}_z} + \sigma^* H_z) \right]$$

$$\frac{\partial \mathbf{H}}{\partial t} = -\frac{1}{\mu} \nabla \times \mathbf{E} - \frac{1}{\mu} (\mathbf{M}_{\text{source}} + \sigma^* \mathbf{H})$$

$$\frac{\partial E_x}{\partial t} = \frac{1}{\varepsilon} \left[\frac{\partial H_z}{\partial y} - \frac{\partial H_y}{\partial z} - (J_{\text{source}_x} + \sigma E_x) \right]$$

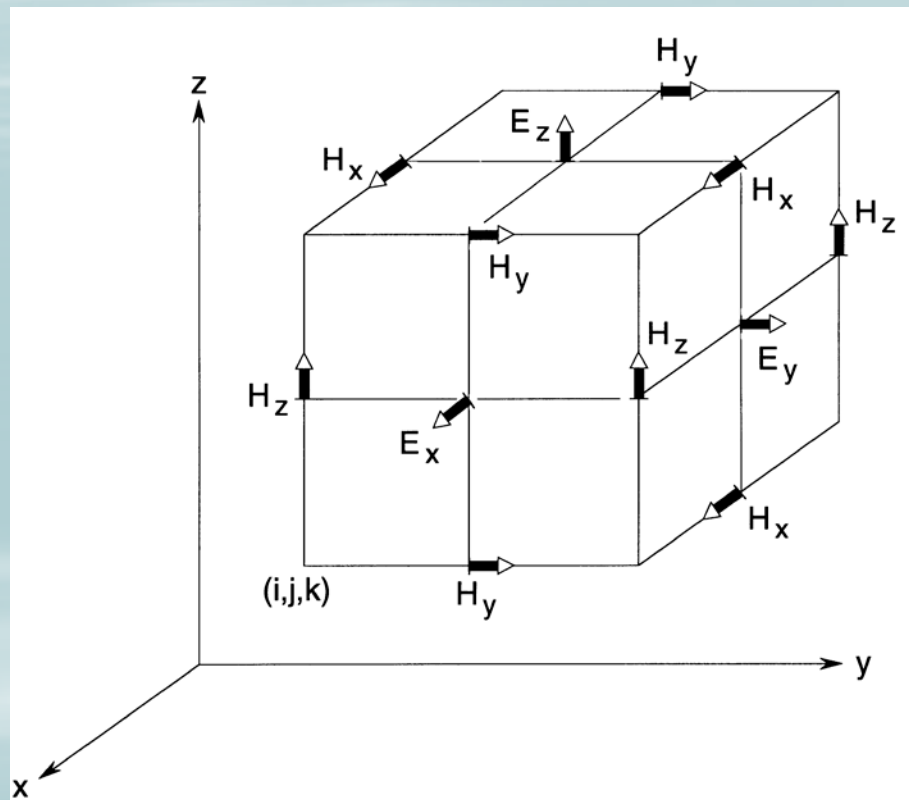
$$\frac{\partial E_y}{\partial t} = \frac{1}{\varepsilon} \left[\frac{\partial H_x}{\partial z} - \frac{\partial H_z}{\partial x} - (J_{\text{source}_y} + \sigma E_y) \right]$$

$$\frac{\partial E_z}{\partial t} = \frac{1}{\varepsilon} \left[\frac{\partial H_y}{\partial x} - \frac{\partial H_x}{\partial y} - (J_{\text{source}_z} + \sigma E_z) \right]$$

$$\frac{\partial \mathbf{E}}{\partial t} = \frac{1}{\varepsilon} \nabla \times \mathbf{H} - \frac{1}{\varepsilon} (\mathbf{J}_{\text{source}} + \sigma \mathbf{E})$$

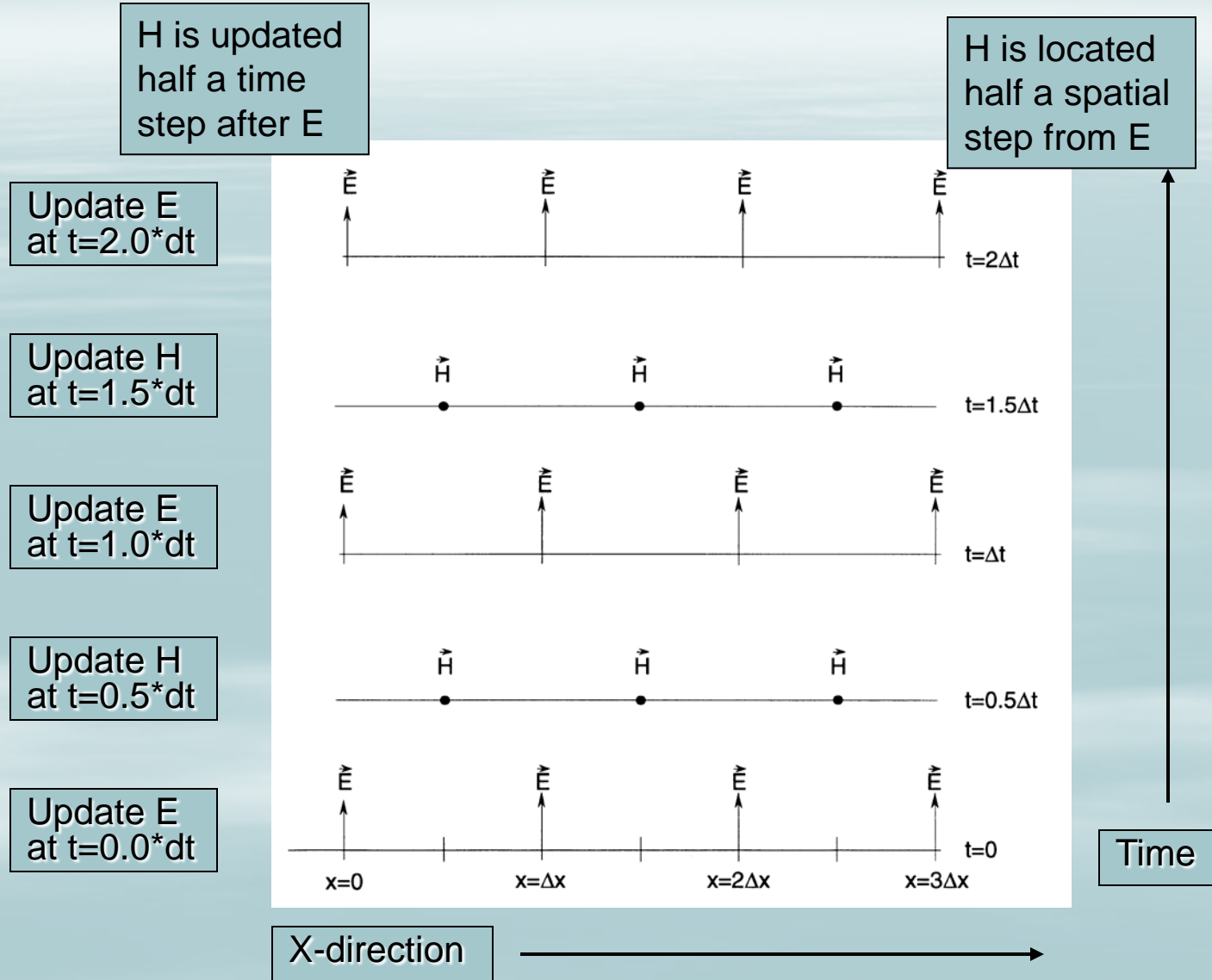
Finite Difference Time Domain 3-D Yee-Cell

Dual spatial grid is commonly used for coupled electric and magnetic fields



H components surrounded by four circulating E fields and vice versa

1-D Time-Step Leapfrog Method



E-field Update Equations

$$\frac{\partial u}{\partial t}(i\Delta x, j\Delta y, k\Delta z, n\Delta t) = \frac{u_{i,j,k}^{n+1/2} - u_{i,j,k}^{n-1/2}}{\Delta t} + O[(\Delta t)^2]$$

FD approximation of the partial derivative of u w.r.t time

$$\frac{\partial E_x}{\partial t} = \frac{1}{\epsilon} \left[\frac{\partial H_z}{\partial y} - \frac{\partial H_y}{\partial z} - (J_{\text{source}_x} + \sigma E_x) \right]$$

Partial derivative of the electric field via Maxwell's equations

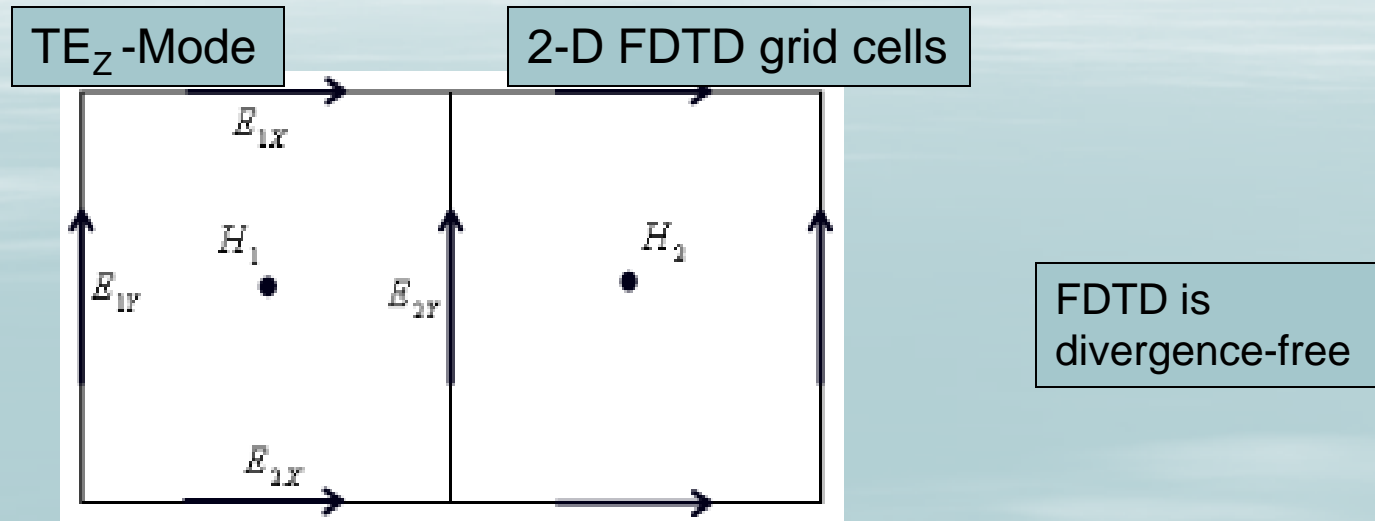
$$\frac{E_x|_{i,j+1/2,k+1/2}^{n+1/2} - E_x|_{i,j+1/2,k+1/2}^{n-1/2}}{\Delta t} =$$

FDTD approximation of the partial derivative of E w.r.t. time

Leapfrog time-stepping

$$\frac{1}{\epsilon_{i,j+1/2,k+1/2}} \cdot \left(\frac{H_z|_{i,j+1,k+1/2}^n - H_z|_{i,j,k+1/2}^n}{\Delta y} - \frac{H_y|_{i,j+1/2,k+1}^n - H_y|_{i,j+1/2,k}^n}{\Delta z} - J_{\text{source}_x}|_{i,j+1/2,k+1/2}^n - \sigma_{i,j+1/2,k+1/2} E_x|_{i,j+1/2,k+1/2}^n \right)$$

2-D FDTD Update



$$E_{2Y}^{n+\frac{1}{2}} = C_1 E_{2Y}^{n-\frac{1}{2}} + \frac{\Delta t \Delta x}{C_2 \epsilon A} (H_1^n - H_2^n)$$

$$H_1^{n+1} = H_1^n + \frac{\Delta t \Delta x}{\mu A} \left(E_{1Y}^{n+\frac{1}{2}} - E_{2Y}^{n+\frac{1}{2}} + E_{1X}^{n+\frac{1}{2}} - E_{2X}^{n+\frac{1}{2}} \right)$$

2-D TM_z Mode

$$E_x = E_y = H_z = 0$$

$$\frac{\partial H_x}{\partial t} = \frac{1}{\mu} \left[-\frac{\partial E_z}{\partial y} - \left(M_{\text{source}_x} + \sigma^* H_x \right) \right]$$

$$\frac{\partial H_y}{\partial t} = \frac{1}{\mu} \left[\frac{\partial E_z}{\partial x} - \left(M_{\text{source}_y} + \sigma^* H_y \right) \right]$$

$$\frac{\partial E_z}{\partial t} = \frac{1}{\varepsilon} \left[\frac{\partial H_y}{\partial x} - \frac{\partial H_x}{\partial y} - \left(J_{\text{source}_z} + \sigma E_z \right) \right]$$

2-D FDTD Update for TM_z Mode

$$H_x|_{i-1/2, j+1}^{n+1} = D_a(m) H_x|_{i-1/2, j+1}^n$$

$$D_a|_{i,j,k} = \left(1 - \frac{\sigma_{i,j,k}^* \Delta t}{2\mu_{i,j,k}} \right) / \left(1 + \frac{\sigma_{i,j,k}^* \Delta t}{2\mu_{i,j,k}} \right)$$

$$+ D_b(m) \cdot \left(E_z|_{i-1/2, j+1/2}^{n+1/2} - E_z|_{i-1/2, j+3/2}^{n+1/2} - M_{\text{source}_x}|_{i-1/2, j+1}^{n+1/2} \Delta \right)$$

$$H_y|_{i, j+1/2}^{n+1} = D_a(m) H_y|_{i, j+1/2}^n$$

$$D_b|_{i,j,k} = \left(\frac{\Delta t}{\mu_{i,j,k} \Delta_1} \right) / \left(1 + \frac{\sigma_{i,j,k}^* \Delta t}{2\mu_{i,j,k}} \right)$$

$$+ D_b(m) \cdot \left(E_z|_{i+1/2, j+1/2}^{n+1/2} - E_z|_{i-1/2, j+1/2}^{n+1/2} - M_{\text{source}_y}|_{i, j+1/2}^{n+1/2} \Delta \right)$$

$$C_a|_{i,j,k} = \left(1 - \frac{\sigma_{i,j,k} \Delta t}{2\varepsilon_{i,j,k}} \right) / \left(1 + \frac{\sigma_{i,j,k} \Delta t}{2\varepsilon_{i,j,k}} \right)$$

$$E_z|_{i-1/2, j+1/2}^{n+1/2} = C_a(m) E_z|_{i-1/2, j+1/2}^{n-1/2} + C_b(m) \cdot \left(H_y|_{i, j+1/2}^n - \right.$$

$$\left. H_y|_{i-1, j+1/2}^n + H_x|_{i-1/2, j}^n - H_x|_{i-1/2, j+1}^n - J_{\text{source}_z}|_{i-1/2, j+1/2}^n \Delta \right)$$

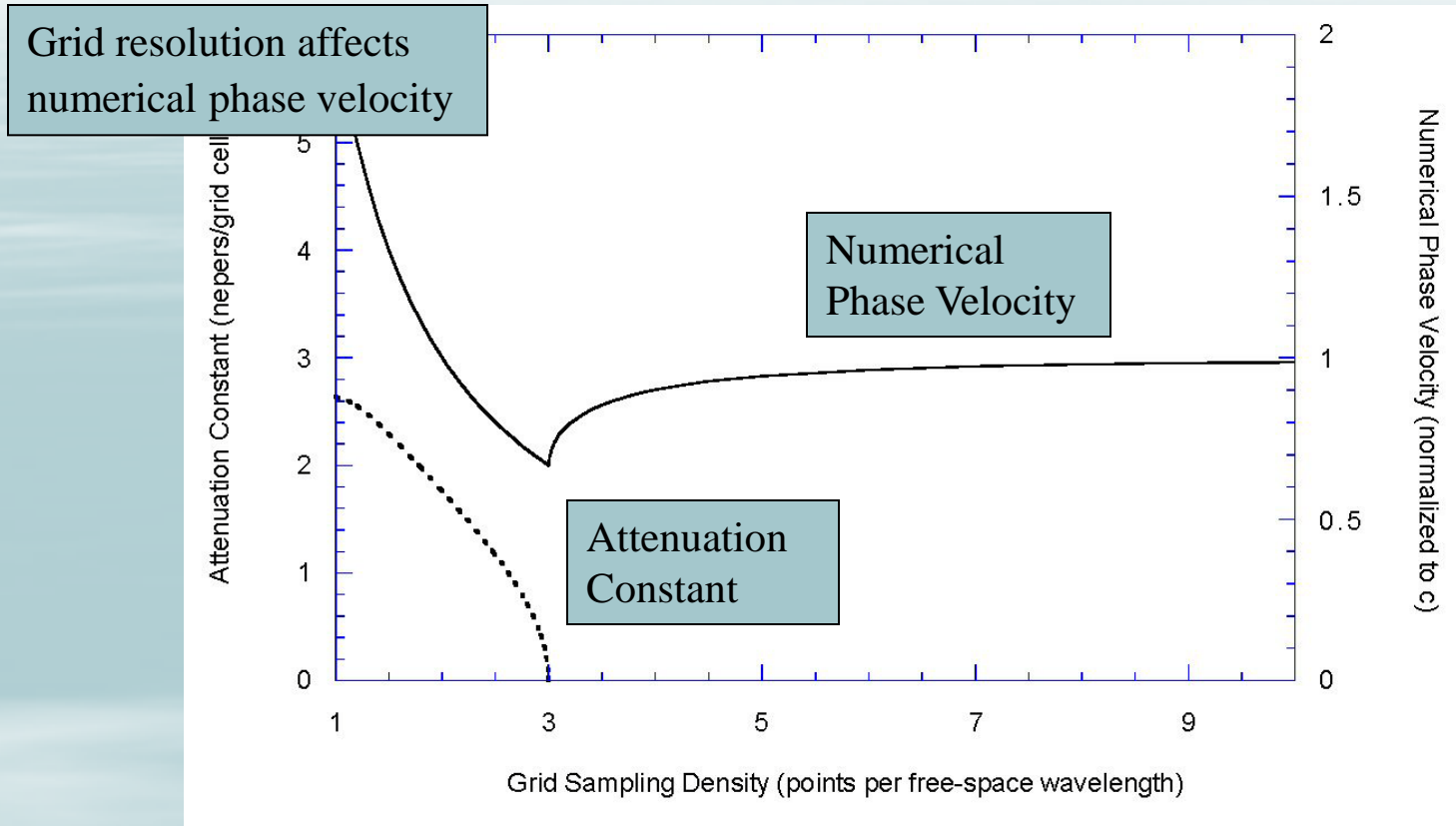
$$C_b|_{i,j,k} = \left(\frac{\Delta t}{\varepsilon_{i,j,k} \Delta_1} \right) / \left(1 + \frac{\sigma_{i,j,k} \Delta t}{2\varepsilon_{i,j,k}} \right)$$

FDTD Considerations

- Grid resolution affects ...
 - Geometry discretization
 - Frequency resolution
 - Numerical phase velocity
 - Accuracy
 - Simulation speed
- Time step affects ...
 - Numerical stability
 - Simulation speed
- Absorbing boundary conditions affects ...
 - Non-physical reflections from computational domain
 - Accuracy
 - Simulation speed and computer memory requirements
- Meshing algorithm (staircased/conformal/nonorthogonal) affects ...
 - Numerical stability
 - Complexity of programming
 - Accuracy
 - Simulation speed and computer memory requirements

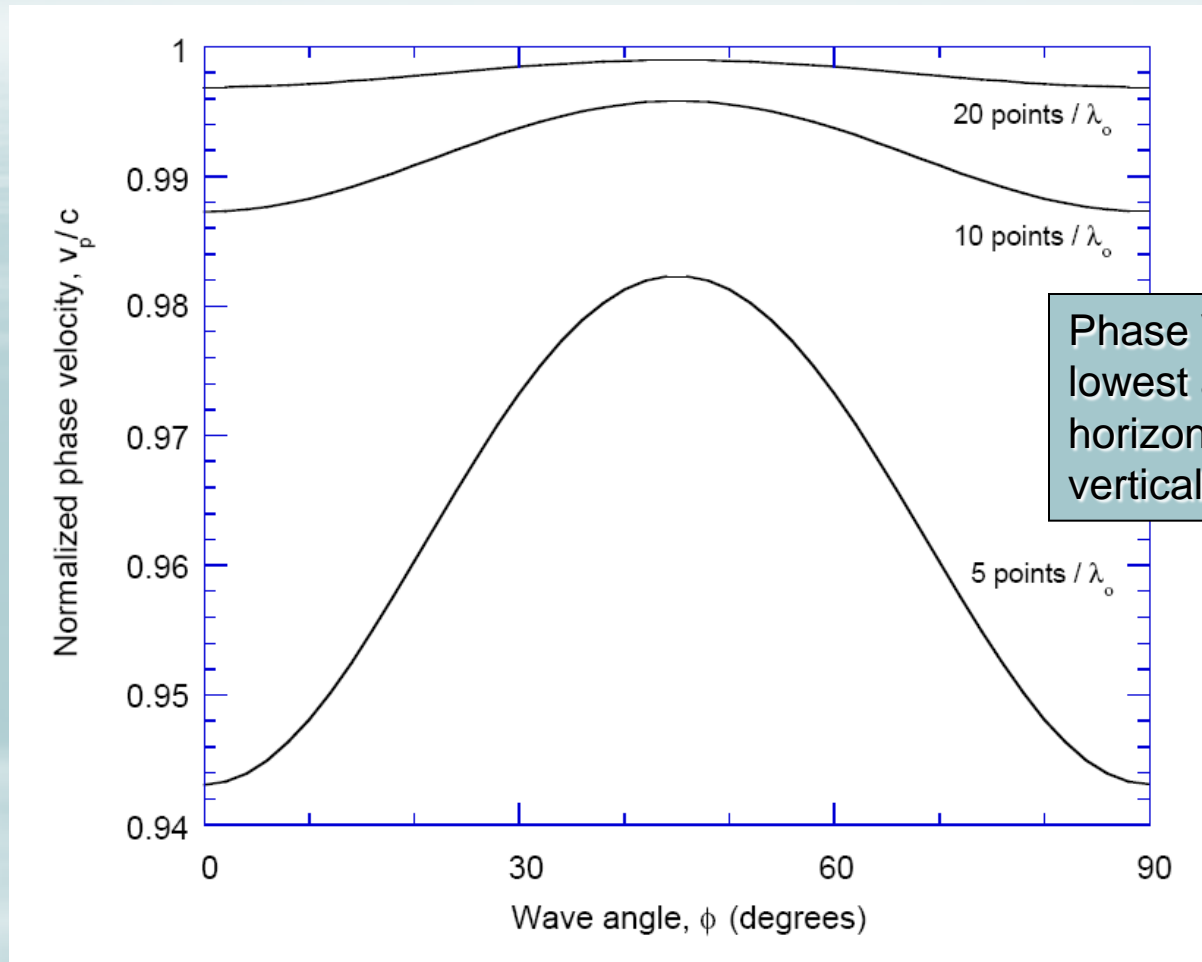
Numerical phase
velocity is anisotropic

FDTD Phase Velocity



Variation of the normalized numerical phase velocity and attenuation per grid cell as a function of the grid sampling density ($1 \leq N \leq 10$) for a Courant stability factor $S = 0.5$

Numerical Phase Velocity Anisotropy



Variation of the numerical phase velocity with wave-propagation angle in a 2-D FDTD grid for three sampling densities of the square unit cells. $S = c \Delta t = 0.5$ for all cases.

Numerical Stability

- Complex issue based on boundary conditions, (un)structured meshing, lossy/dispersive materials.
- Courant condition must be satisfied in all cases that we will consider

1-d

$$\Delta t = \frac{\Delta x}{c}$$

2-d

$$\Delta t = \frac{\Delta x}{c\sqrt{2}}$$

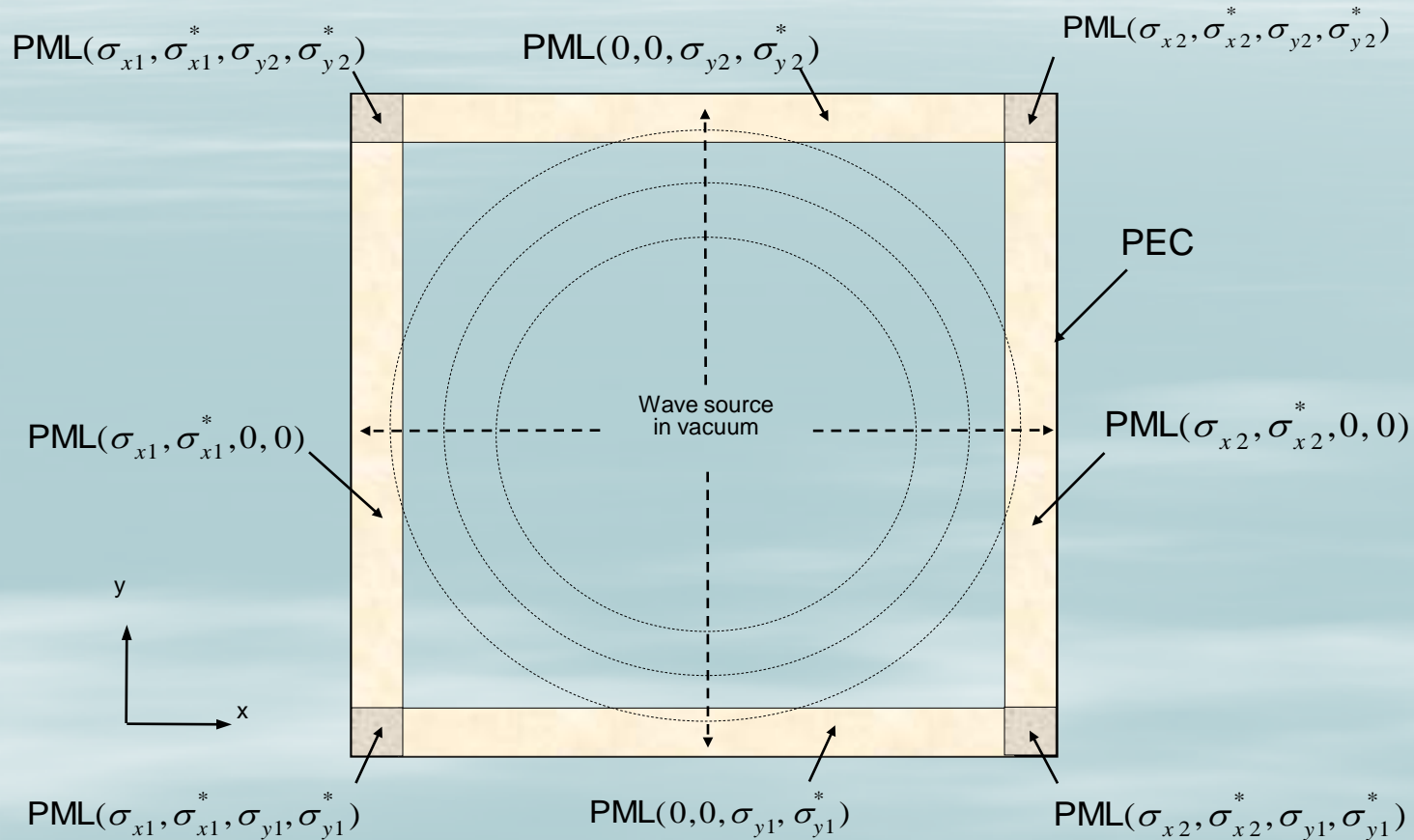
3-d

$$\Delta t = \frac{\Delta x}{c\sqrt{3}}$$

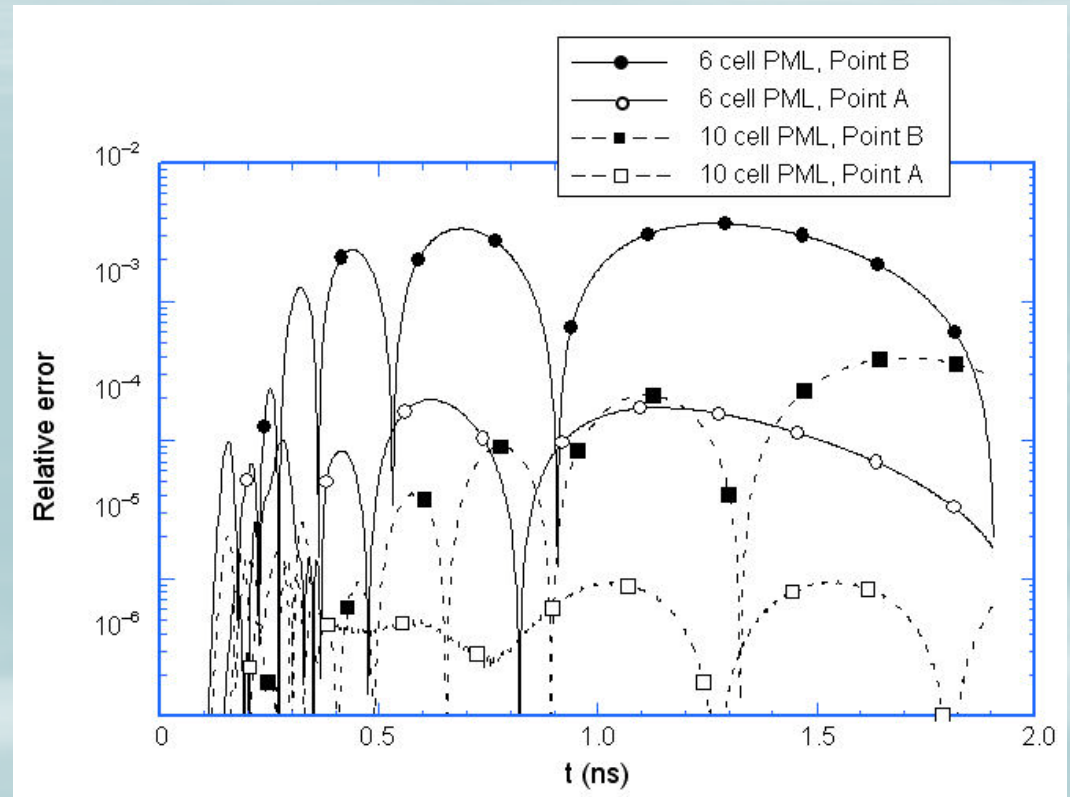
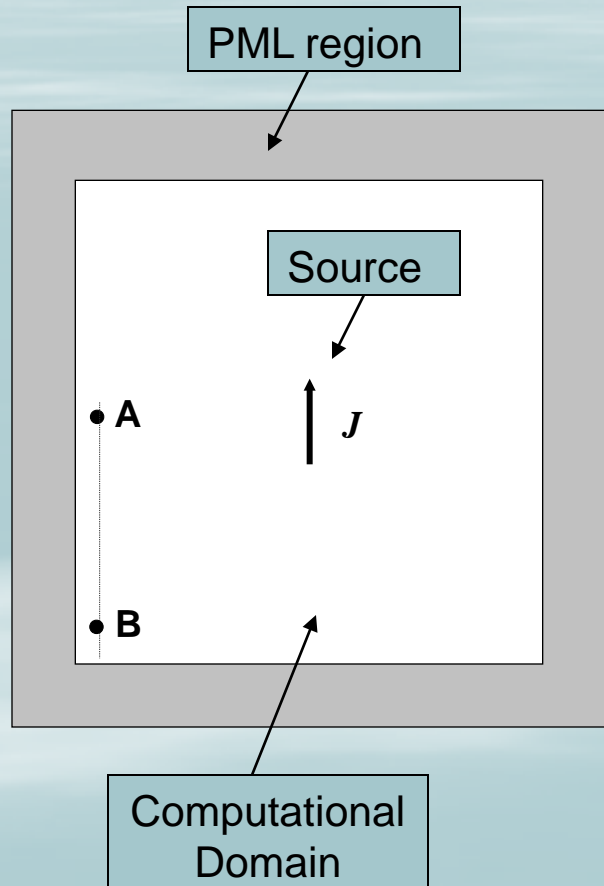
Δx is the smallest mesh cell in the FDTD grid

1-d interpretation: Field energy may not transit through more than one complete mesh cell in a single time-step

Perfectly Matched Layer (PML)

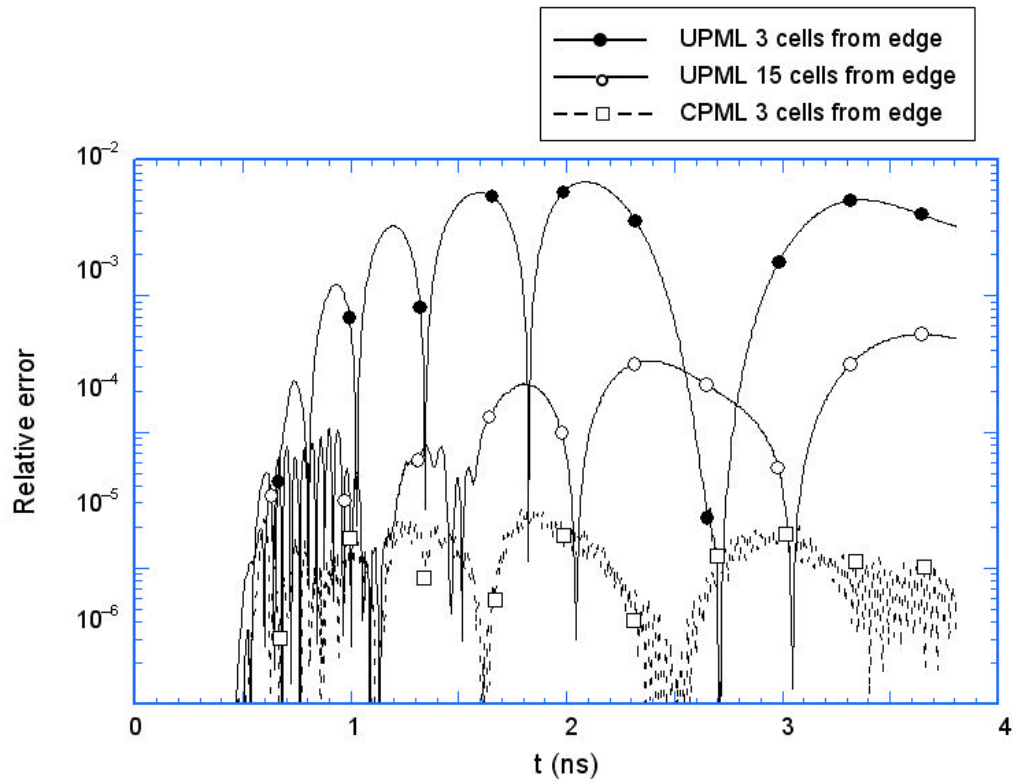
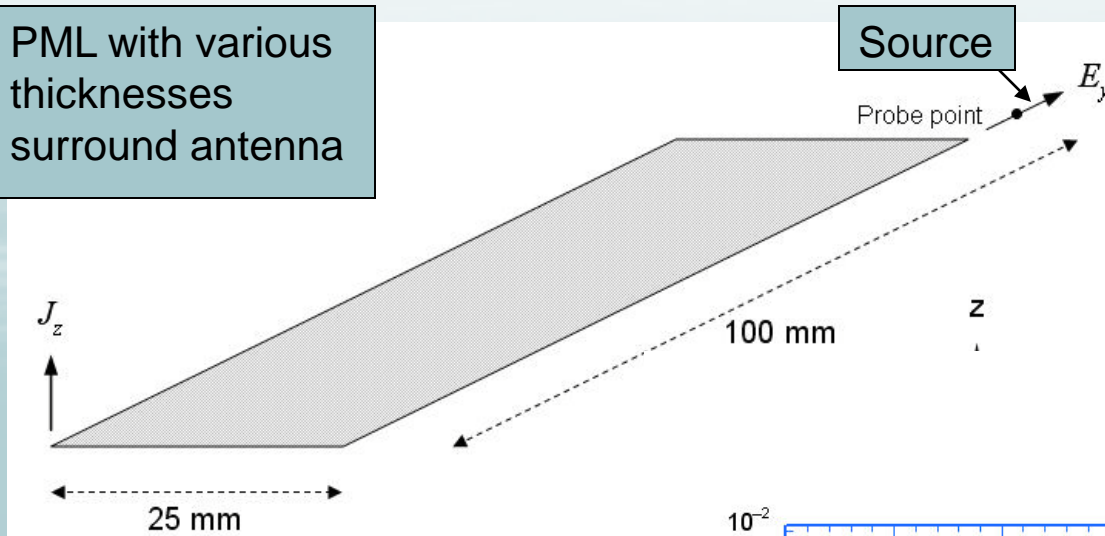


PML: Wave Incidence Angle



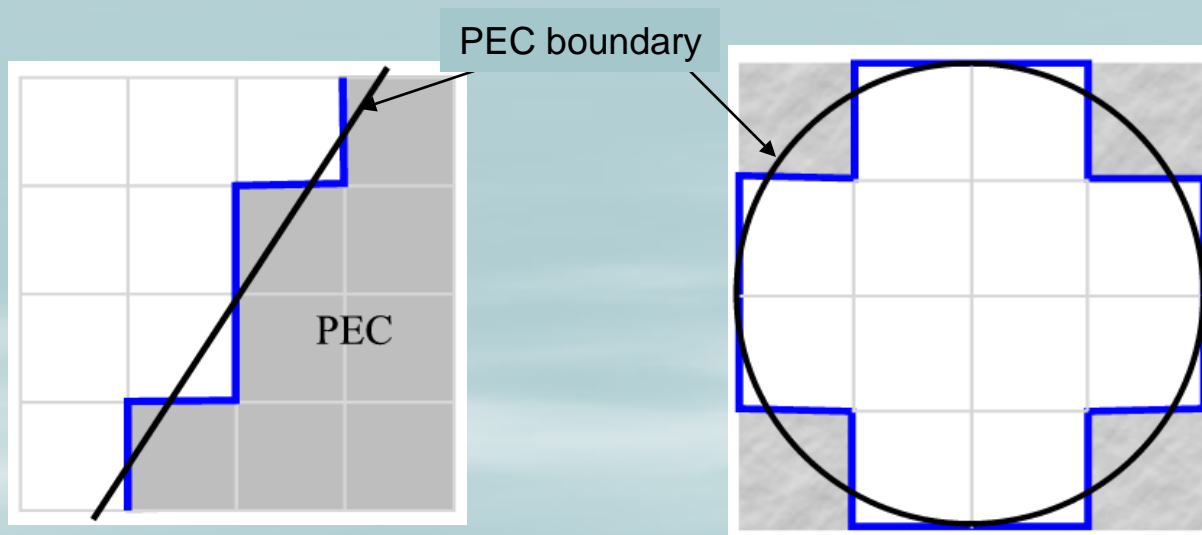
PML Thickness

PML with various thicknesses surround antenna



FDTD Geometry Staircasing

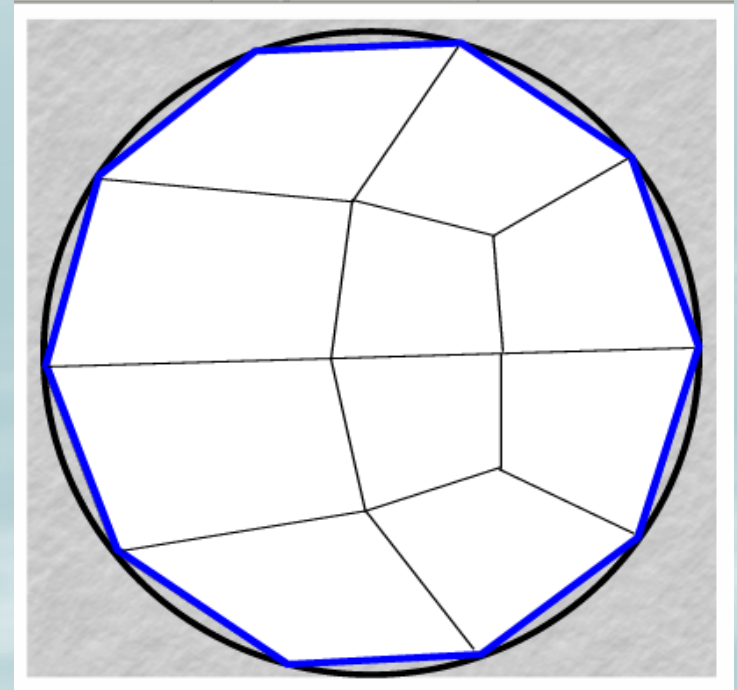
- Significant deformations of the original geometry
- Inflexible meshing capabilities
- Standard FDTD edge is a single material
- FDTD grid cell is entirely inside or outside material



$O(n^2)$ accuracy does not include meshing inaccuracies

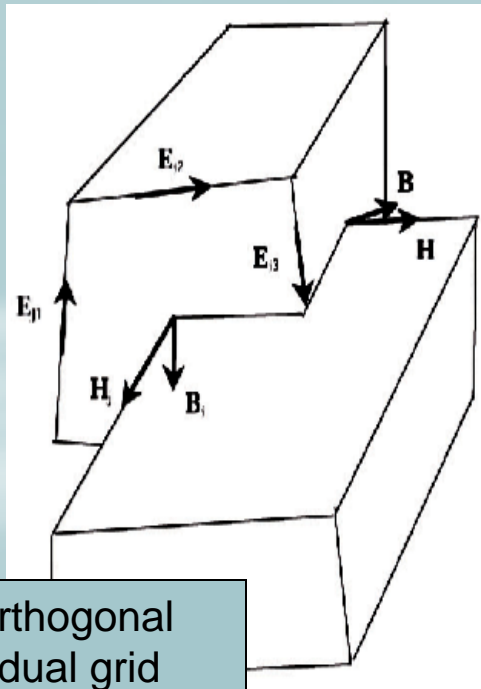
Non-Orthogonal Mesh

- Irregular, non-orthogonal grids offer the greatest geometric flexibility
- Finite element meshing algorithm
- Pre-existing reliable mesh generators from CFM solvers
- Maps boundaries much more precisely without requiring dense mesh
- Permits modeling of arbitrary objects with fine spatial features
- Reduces solution time due to fewer mesh cells
- No regular meshing structure necessitates complex methodology



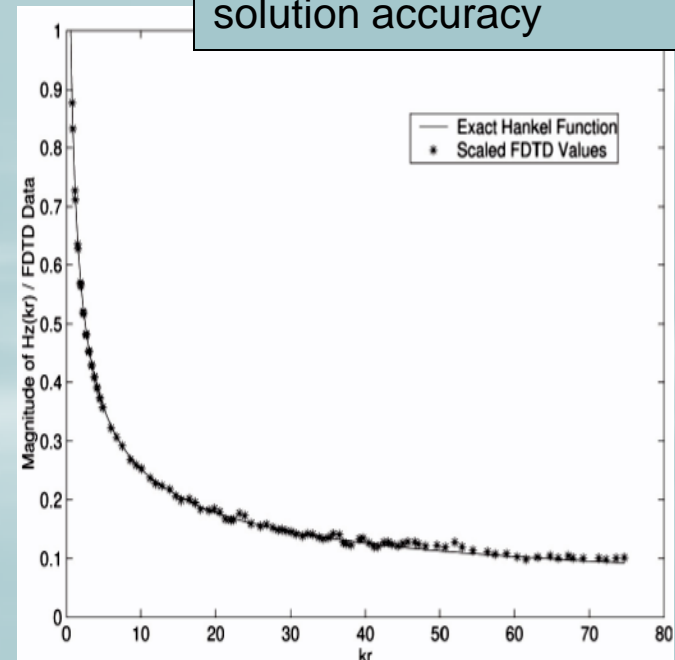
Non-Orthogonal Algorithm

- B is orthogonal to cell face and is calculated from Maxwell's equations
- H is collinear with cell edge and requires a projection operation
- Vector sum of B fields is calculated and averaged on the corners
- Resultant B field is projected onto non-orthogonal cell edge
- Unstable algorithm stabilized by creating a symmetric matrix update
- Non-physical term added to update eqns. degrades accuracy



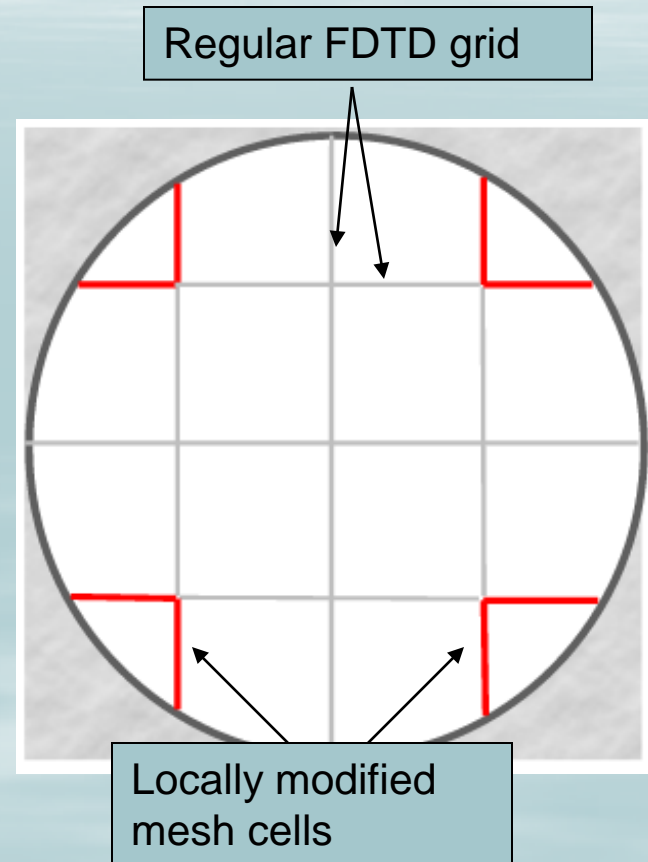
Non-orthogonal
mesh dual grid

Irregular mesh degrades
solution accuracy



Locally Conformal Method

- Locally conformal meshes are the most reliable and proven methods
- Alters existing orthogonal FDTD grid
- Modifies edge lengths and areas only at intersection points
- Remainder of FDTD grid undisturbed
- Easy to implement with current FDTD electromagnetic solvers
- Difficult mesh generation



CP-FDTD Update Equations

- Typical update

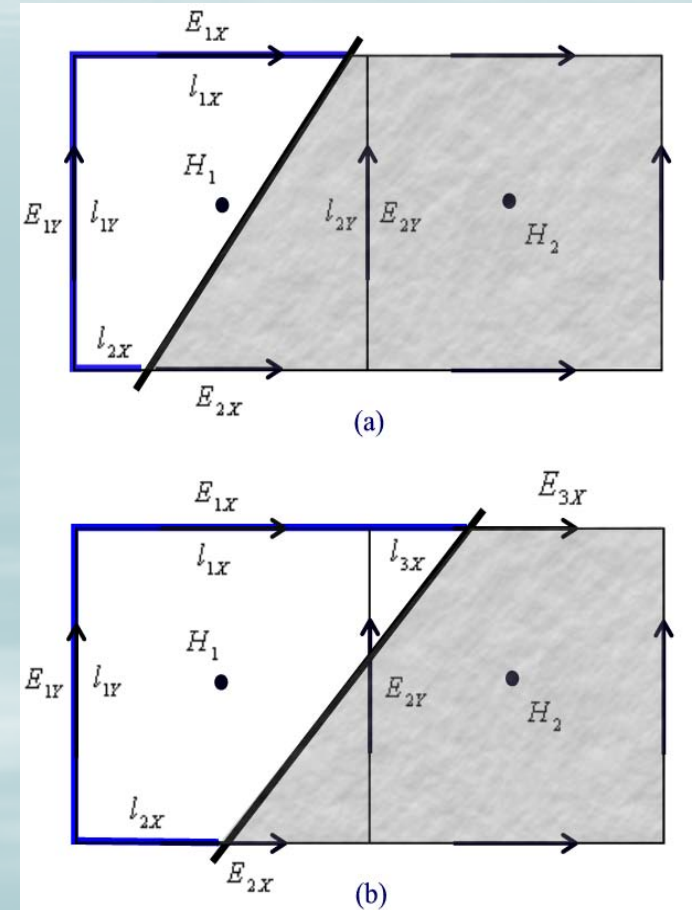
$$H_1^{n+1} = H_1^n + \frac{\Delta t}{\mu A_1} \left(\begin{array}{l} E_{1Y}^{n+\frac{1}{2}} * l_{1Y} - E_{2Y}^{n+\frac{1}{2}} * l_{2Y} \\ + E_{1X}^{n+\frac{1}{2}} * l_{1X} - E_{2X}^{n+\frac{1}{2}} * l_{2X} \end{array} \right)$$

- Cell expansion

$$H_1^{n+1} = H_1^n + \frac{\Delta t}{\mu(A_1 + A_2)} \left(\begin{array}{l} E_{1Y}^{n+\frac{1}{2}} * l_{1Y} - E_{2X}^{n+\frac{1}{2}} * l_{2X} + \\ E_{1X}^{n+\frac{1}{2}} * (l_{1X} + l_{3X}) \end{array} \right)$$

$$E_{3X} = E_{1X}$$

- Instability issues resolved, but somewhat difficult to implement – simpler solutions exist.



Contour-Path Method, Jurgens and Taflove

D-FDTD Update Equations

- Typical update

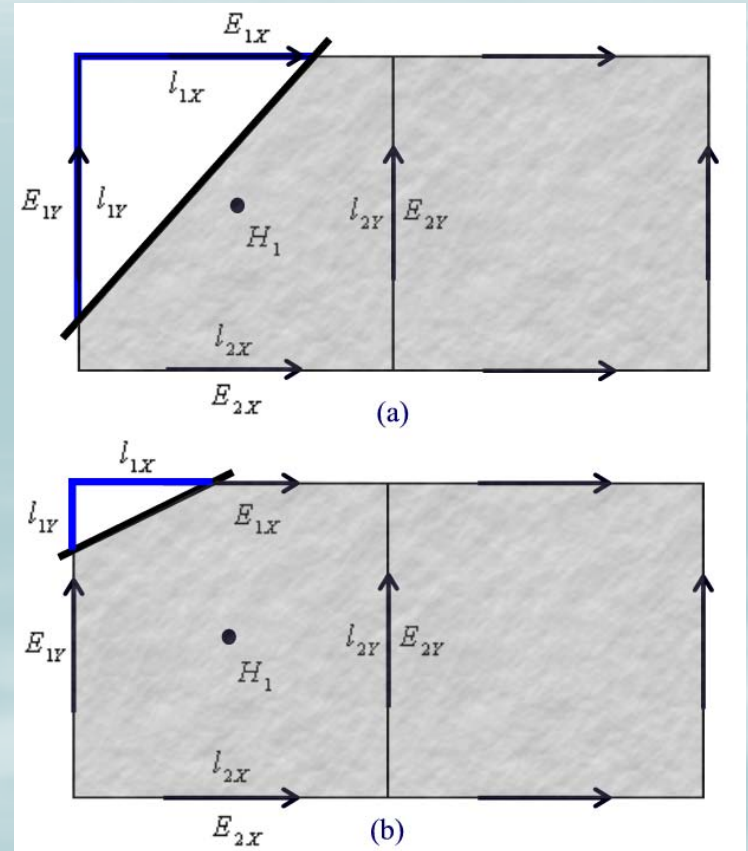
$$H_1^{n+1} = H_1^n + \frac{\Delta t}{\mu A_1} \begin{pmatrix} E_{1Y}^{n+\frac{1}{2}} * l_{1Y} - E_{2Y}^{n+\frac{1}{2}} * l_{2Y} \\ + E_{1X}^{n+\frac{1}{2}} * l_{1X} - E_{2X}^{n+\frac{1}{2}} * l_{2X} \end{pmatrix}$$

- Stability criterion violated

$$E_{1Y}^{n+\frac{1}{2}} = E_{2Y}^{n+\frac{1}{2}} = E_{1X}^{n+\frac{1}{2}} = E_{2X}^{n+\frac{1}{2}} = 0$$

Stability criterion restricts minimum cell area and maximum ratio of edge length to area.

D-FDTD reduces the number of mesh cells and does not severely effect the minimum time step.



Dey-Mittra FDTD (D-FDTD) method for PEC (IEEE MGW Letters September, 1997)

Field Leakage

- Special consideration must be made to account for field leakage since grid edges do not lie along surface of geometry as in a non-orthogonal grid.

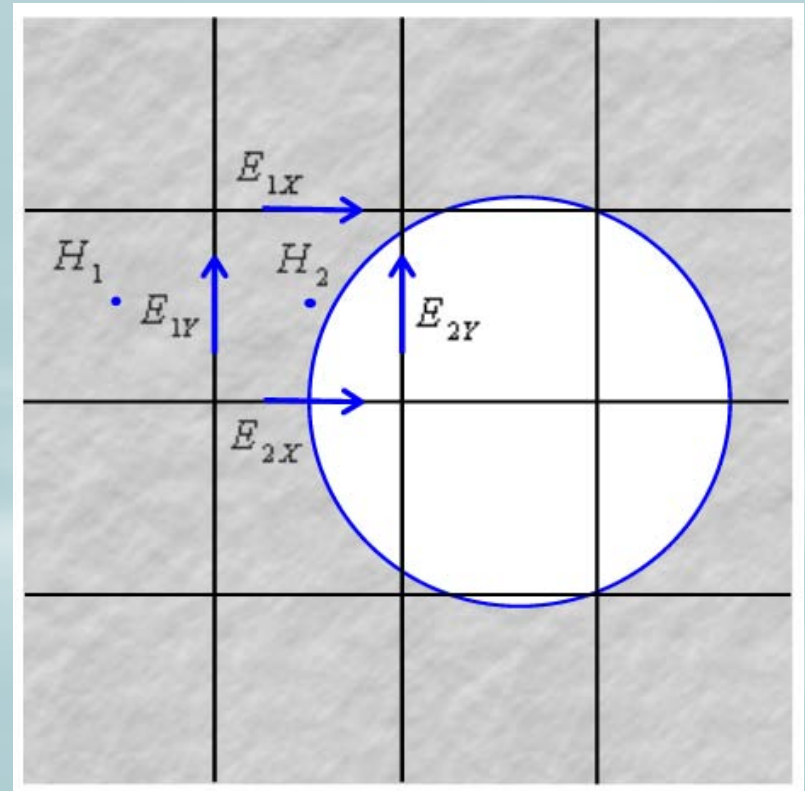
Partial edge lengths allow fields to pass through boundary of geometry into PEC

- D-FDTD update equation for H2

$$H_2^{n+1} = H_2^n - \frac{\Delta t}{\mu A_1} \left(E_{2Y}^{n+\frac{1}{2}} * l_{2Y} + E_{2X}^{n+\frac{1}{2}} * l_{2X} \right)$$

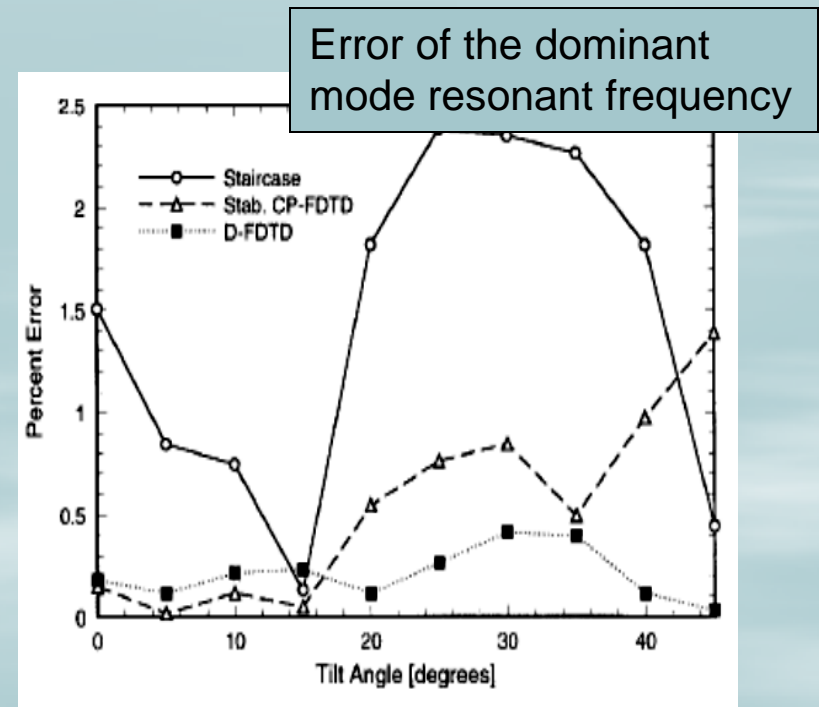
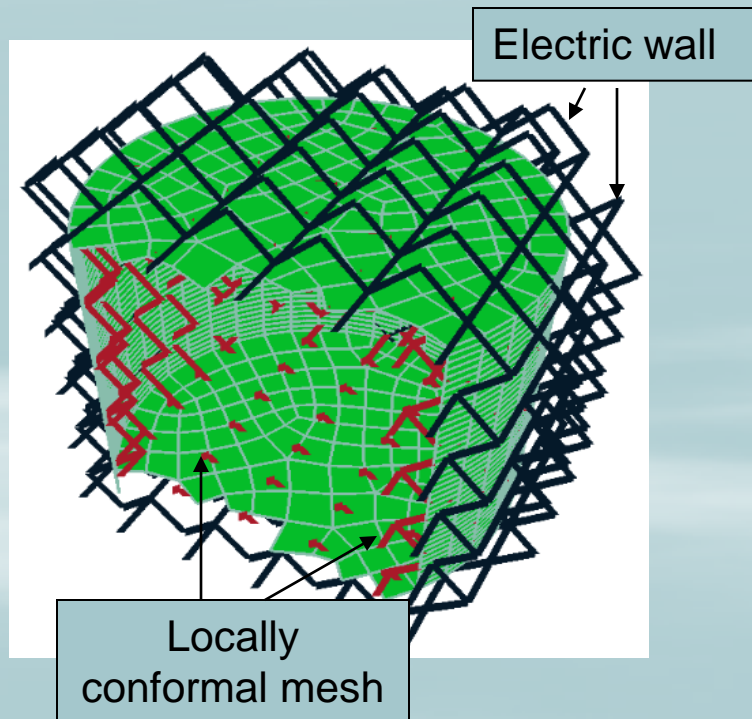
- D-FDTD update for E1Y in the PEC

$$E_{1Y}^{n+\frac{1}{2}} = E_{1Y}^{n-\frac{1}{2}} + \frac{\Delta t}{\epsilon \Delta x} (H_1^n - H_2^n)$$



D-FDTD Results

- 3-D cylindrical resonator tilted at angles ranging from 0 to 45 degrees in the FDTD grid is compared with simple staircased mesh.



(IEEE MTT Railton C., Schneider J., Jan., 1999)

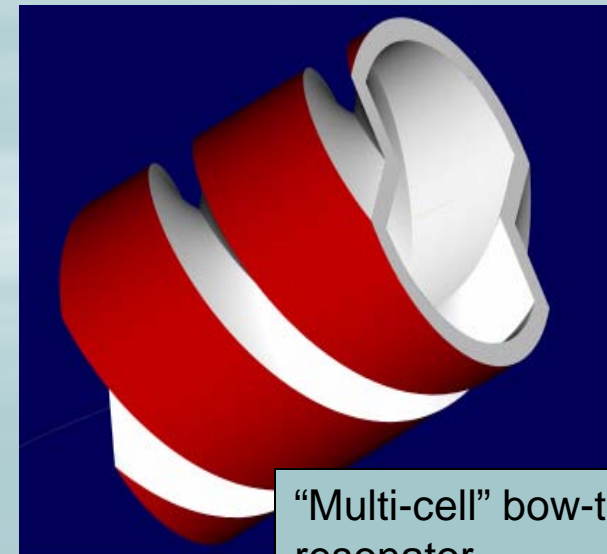
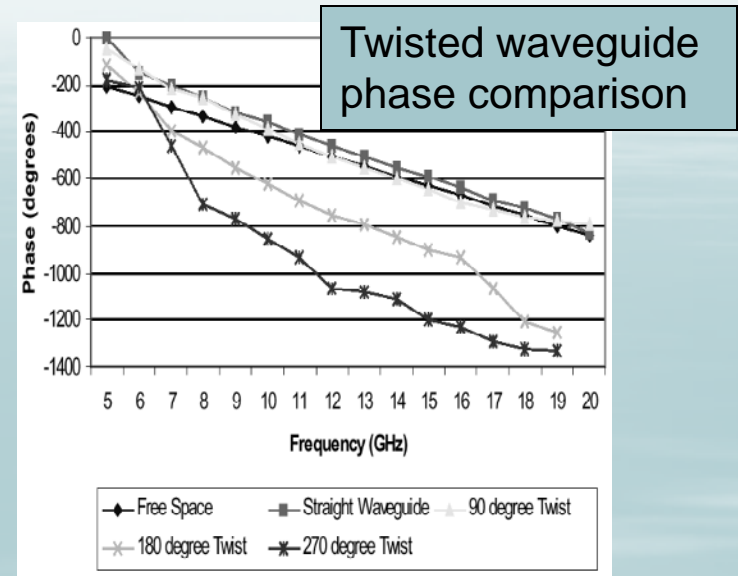
Slow-wave Structures: Twisted Resonators

- Slow-wave structure can be designed by twisting waveguide.
- Phase velocity can be controlled by pitch of the twist.

Floquet's theorem explicitly shows the relationship with the fields at a given location in a periodic structure to the fields a period away.

$$\vec{E}(r, z, t) = \sum_{n=-\infty}^{\infty} a_n(r) e^{j\left(\beta_0 + \frac{2\pi n}{L}\right)z} e^{j\omega t}$$

$$\vec{E}_z(r, z, t) = \sum_{n=-\infty}^{\infty} E_n J_0(K_n r) e^{j(\omega t - \beta_n z)}$$

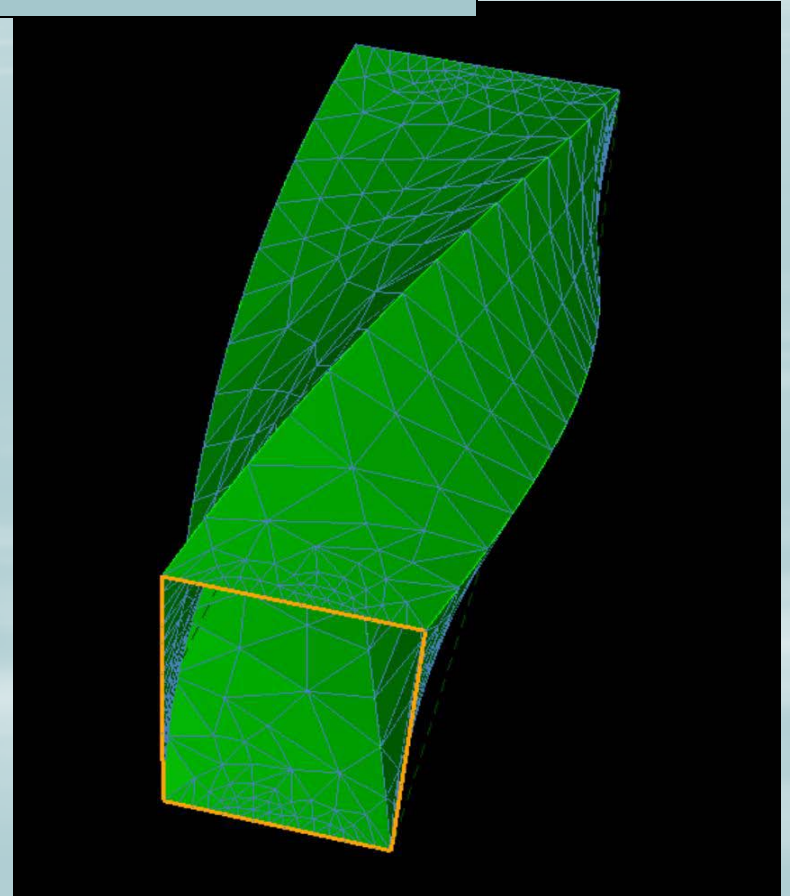
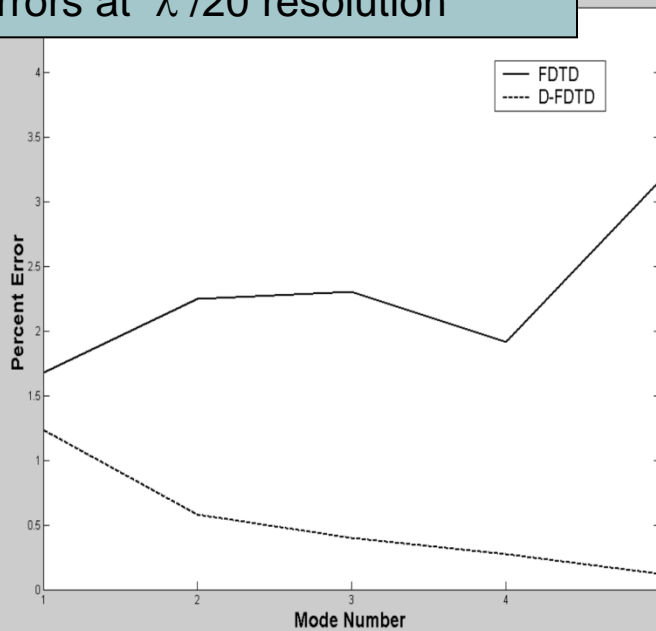


"Multi-cell" bow-tie resonator

Twisted Resonator: Rectangular

Twisted rectangular resonator

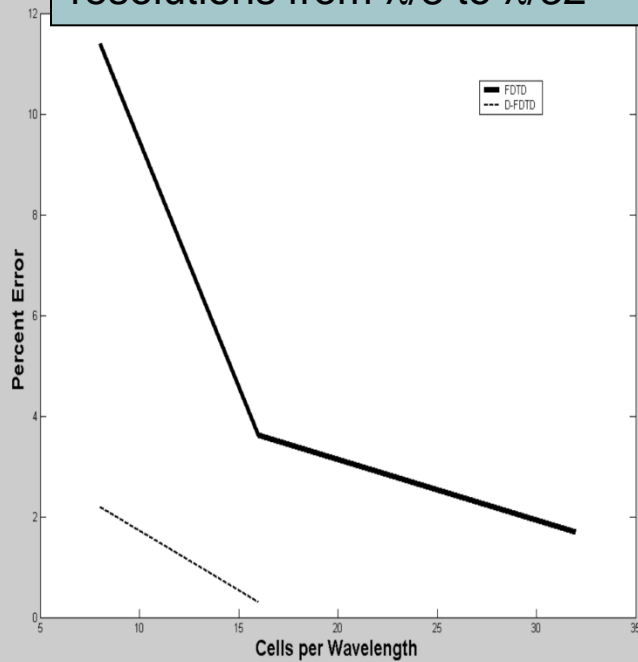
Fundamental and higher order mode resonant frequency errors at $\lambda/20$ resolution



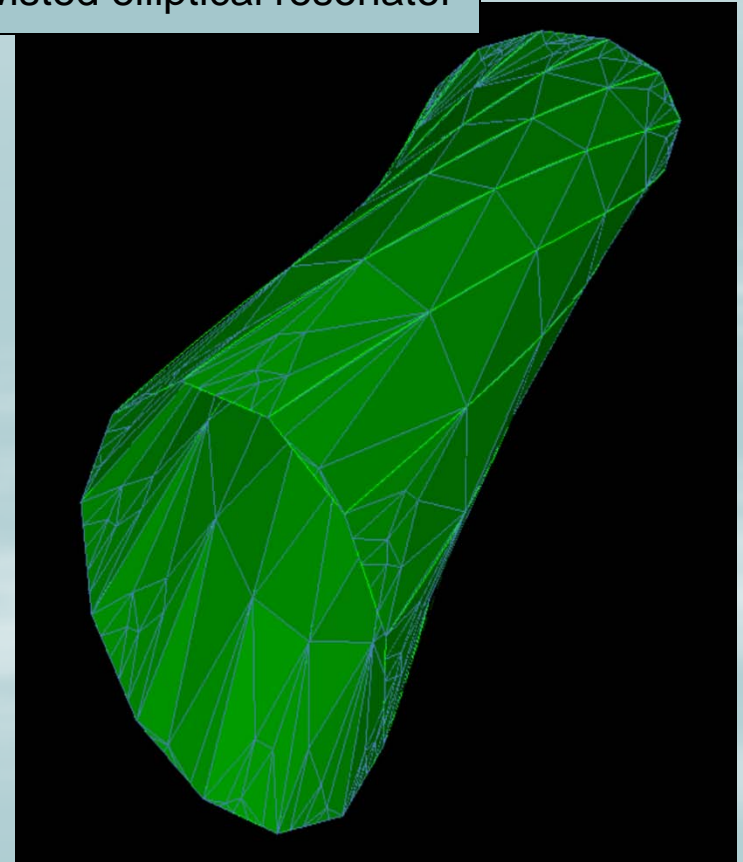
Twisted Resonator: Elliptical

- Elliptical cross-section not easily meshed with cubical FDTD grid
- Conformal algorithms well suited to geometry

Fundamental mode resonant frequency error with grid resolutions from $\lambda/8$ to $\lambda/32$



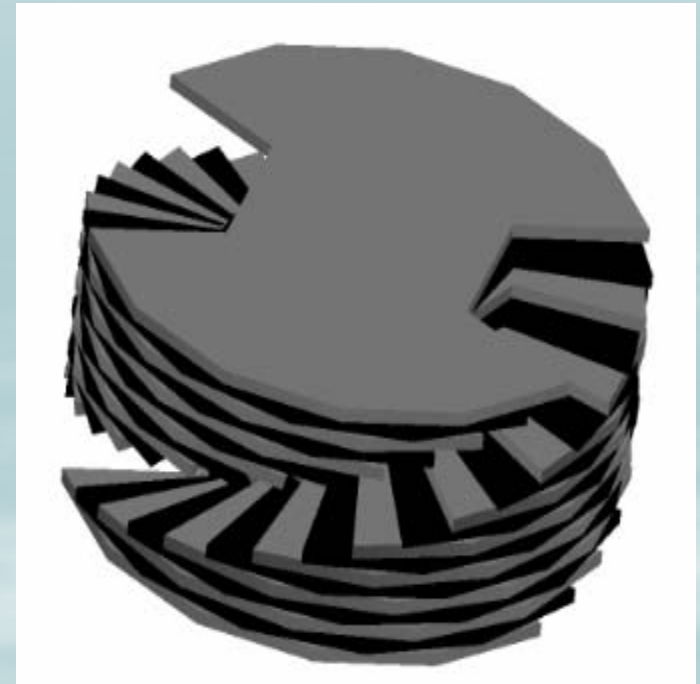
Twisted elliptical resonator



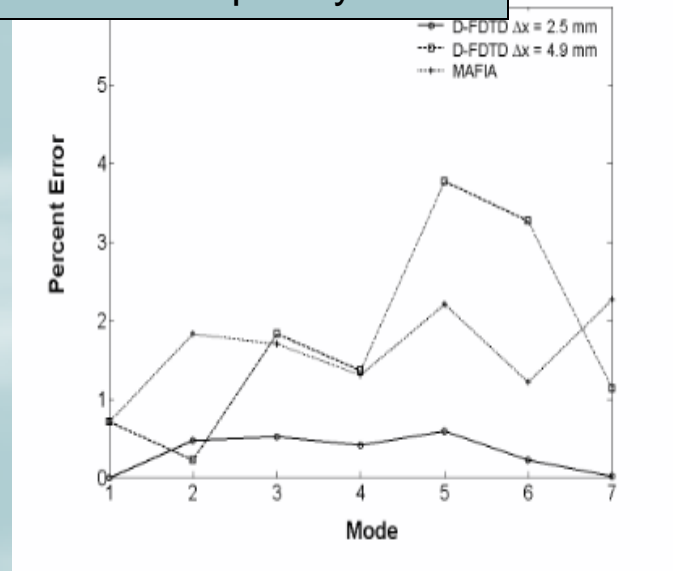
Twisted Resonator: Stacked Cylindrical Notch

- MAFIA™ does not use conformal meshing algorithm.
- Smoothly twisted waveguide can not be modeled by staircasing.
- Stacked disk, twisted waveguide approximates actual design

Stacked notch resonator



Fundamental and higher order mode resonant frequency errors



Twisted Resonator: Smooth Notch

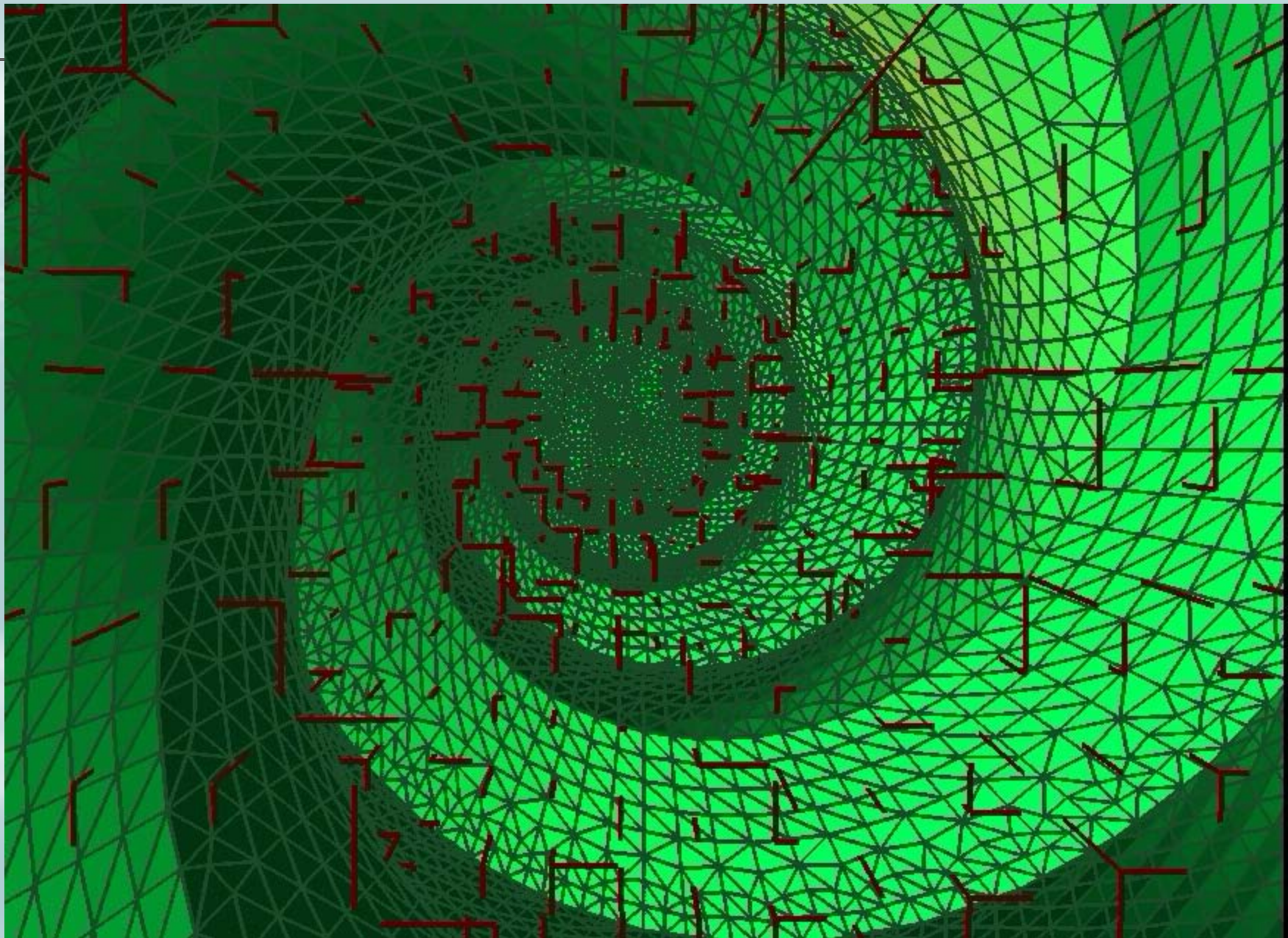
- Requires a conformal algorithm to model accurately.
- FEA and locally conformal meshes can be used to evaluate actual waveguide geometry.
- Typical mesh in D-FDTD for a four-period twisted notched waveguide included 50,000 modified FDTD grid edges.
- Mesh created in 5 minutes.
- Efficient and accurate results.

FEA solver HFSS™ v. 8.0 required 500 MB of memory and 4 hours for the solution of a 3-period twisted waveguide to retrieve 20 modes.

Single-period notched resonator



D-FDTD requires 20 MB of memory and 30 minutes for the same solution and retrieved frequency data across 5 GHz bandwidth.



USPAS June 2010

HMWK

- Write a Matlab or C-program that models 1-D x-directed plane-wave propagation in a uniform FDTD Yee grid using the necessary 2-D equations described for the TMz mode (assume $H_x=0$).
 - Assume material with $\sigma=1e-3$, and use the time step $dt=dx/c$.
 - Terminate the grid in Ez components at its far-left and far-right boundaries.
 - Source the grid with an Ez field at the far-left boundary with a 1GHz sinusoid to create a rightward-propagating wave.
 - Set $E_z=0$ at the far-right boundary to simulate PEC. Perform visualizations of the field components within the grid at a number of time snapshots before and after the propagating wave reaches the far-right grid boundary.
 - Set the time step to $dt=1.01*dx/c$. Compare results.
 - Repeat the previous experiment using $H=0$ at the right boundary and note the differences.